Polyelectrolyte−Micelle Coacervation: Effects of Micelle Surface Charge Density, Polymer Molecular Weight, and Polymer/Surfactant Ratio

Yilin Wang, Kozue Kimura, and Paul L. Dubin*

Department of Chemistry, Indiana University-Purdue University, Indianapolis, Indiana 46202

Werner Jaeger

Fraunhofer-Institut fur Angewandte Polymerforschung, D-14513 Teltow, Germany

Received November 8, 1999; Revised Manuscript Received January 24, 2000

ABSTRACT: The effects of micelle charge density, polymer molecular weight, and polymer-to-surfactant ratio on coacervation were studied by turbidity, dynamic light scattering, and electrophoretic mobility in the system composed of the strong cationic polymer poly(diallyldimethylammonium chloride) (PDADMAC) and oppositely charged mixed micelles of Triton X-100 (TX100) and sodium dodecyl sulfate (SDS). Phase boundaries in the range of SDS mole fraction from 0.30 to 0.50 and in the range of polymer molecular weight from 8.2×10^3 to 4.28×10^5 were obtained, and coacervate volume fraction as a function of polymer molecular weight was subsequently determined. Three-dimensional phase boundaries were used to represent the effects on coacervation of micelle surface charge density, polymer molecular weight, and PDADMAC-to-SDS ratio. The coacervation region is seen to increase with micelle surface charge density and polymer molecular weight (MW). Both higher and lower polyelectrolyte-to-surfactant ratio can suppress coacervation. An increase in MW reduces the micelle charge required for coacervation and also increases coacervate volume fraction. Coacervation is found to occur when the following conditions are satisfied: the electrophoretic mobility is close to zero, and the size of polyelectrolyte−micelle complex is at least about 45 nm.

Introduction

Polyelectrolytes interact strongly with oppositely charged micelles in aqueous systems, normally leading to phase separation:[1−4] liquid−liquid phase separation (coacervation) or liquid−solid phase separation (precipitation). These phase separation phenomena have received growing interest for both theoretical and technological reasons.[4−10]

Coacervation is a phenomenon in which a macromolecular aqueous solution separates into two immiscible liquid phases. The more dense phase, which is relatively concentrated in macromolecules, is called the coacervate and is in equilibrium with the relatively dilute macromolecular liquid phase.[11] For polyelectrolyte−surfactant systems, coacervation, i.e., associative phase separation,[12] yields a phase rich in both polymer and surfactant.[1,12] Both the conditions for coacervation and the coacervate volume fraction are of importance in applications such as cosmetic formulations[13] and pharmaceutical microencapsulation.[14,15]

Polyelectrolyte−micelle coacervation is influenced by many factors. Among these are polymer properties, such as linear charge density, molecular weight (MW), concentration, and molecular geometry; micelle properties such as surface charge density (σ), size, and concentration; and polymer-to-surfactant ratio, ionic strength, and temperature.[1,4,16] All these factors mutually control coacervation. We focus here on micelle surface charge density, polymer MW, and polymer-to-surfactant ratio.

These three factors are of particular interest for several reasons. As indicated previously,[17−19] macromolecular charge density is the most significant factor affecting complex coacervation. At very low charge densities, coacervation is suppressed,[16] and at very high charge densities, precipitation may occur.[16,20] Consequently, micelle surface charge density σ is a critical variable. With regard to polyelectrolyte MW, Voorn and Overbeek[21] predicted an increase in coacervation as the molecular weights of biopolymers increase. Thalberg, Lindman, and co-workers[22] studied the effect of the molecular weight of the polysaccharide hyaluronan (NaHy) on the phase behavior of its mixtures with alkyltrimethylammonium bromide (C_nTAB). The tendency toward phase separation increased slightly with increasing MW, while the size of the two-phase (coacervation) region was little affected. Dubin and coworkers[23] studied complex formation between poly(diallyldimethylammonium chloride) (PDADMAC) and oppositely charged mixed micelles of Triton X-100 (TX100) and sodium dodecyl sulfate (SDS). The results indicated that increasing MW enhances the tendency of interpolymer (vs intrapolymer) complex formation, and they considered the interpolymer complex to be the precursor of complex coacervation. Such results suggest that a minimum polymer molecular weight is required for complex coacervation. Stoichiometry, i.e., polymer-to-surfactant ratio, is also a factor that influences intra- vs interpolymer complex formation. Goddard and Hannan[6,24] found the two-phase region in mixtures of alkyl sulfates and a cationically modified cellulose to be centered around 1:1 polymer-to-surfactant charge ratio. In contrast, Thalberg et al.[25] found for the system hyaluronan (NaHy) and dodecyltrimethylammonium (DTAB) a two-phase region centered around a DTA^+:Hy^- ratio >1, indicating the importance of structural effects.

Micelle surface charge density, polymer MW, and polymer-to-surfactant ratio r are thus very important in coacervation, but the interrelationship among these

10.1021/ma991886y CCC: $19.00
Published on Web 04/12/2000

factors is unclear. It is of considerable interest and usefulness to improve our understanding of coacervation by investigating these factors.

The PDADMAC/TX100-SDS system provides a model system by means of which conjoint effects of σ, MW, and r on coacervation can be studied over a wide range of conditions. This system has been studied by many experimental methods, including turbidimetry,[17,26] dynamic and static light scattering,[23,27,28] viscometry,[28] electrophoretic light scattering,[28] microcalorimetry,[29] dye solubilization,[30] and equilibrium dialysis.[28] These studies revealed the existence of several phase states, including soluble complexes, coacervate, and precipitates, depending inter alia on the mixing ratio of PDADMAC and TX100-SDS. When the charge density of the mixed TX100-SDS micelles is adjusted (via the mole ratio of ionic-to-nonionic surfactant), coacervation is found to exist over a wide range of conditions. This facilitates a systematic study of the relationship among σ, MW, and r.

Experimental Section

Materials. Poly(diallydimethylammonium chloride) (PDADMAC) was prepared by free radical aqueous polymerization of diallydimethylammonium chloride.[31] The average molecular weights (M_n) of the purified lyophilized polymer were determined by membrane osmometry as 8.2×10^3, 3.0×10^4, 5.8×10^4, 9.8×10^4, 1.25×10^5, 1.60×10^5, 1.80×10^5, 2.16×10^5, 2.40×10^5, 2.70×10^5, 3.00×10^5, 4.28×10^5, and 4.60×10^5. Triton X-100 (TX100) was purchased from Aldrich, sodium dodecyl sulfate (SDS, purity >99%) from Fluka, and NaCl from Fisher. All were used without further purification. Distilled water was used in all experiments.

Turbidimetric Titrations. Turbidity measurements, reported as 100 − %T, were performed at 420 nm using a Brinkman PC800 probe colorimeter equipped with a 2 cm path length fiber-optics probe at 26 ± 1 °C. Turbidimetric "type 1" titrations were carried out by adding 60 mM SDS in 0.40 M NaCl to solutions of TX100 and PDADMAC with initial concentration of 20 mM and 1 g/L also in 0.40 M NaCl concentration, to bring the solutions to different Y values. Y is a SDS mole fraction defined as

$$Y = \frac{[\mathrm{SDS}]}{[\mathrm{SDS}] + [\mathrm{TX100}]} \tag{1}$$

which is proportional to the average mixed-micelle surface charge density. Turbidimetric "type 3" titrations were carried out by addition of concentrated PDADMAC in 0.40 M NaCl to a solution of 20 mM TX100 and SDS at constant Y ($Y = 0.30$, 0.35, 0.40, 0.50), also in 0.40 M NaCl. All measured values were corrected by subtracting the turbidity of a polymer-free blank. Turbidity values were recorded when the meter response was constant for 2 min. The time required to reach this equilibrium varied from 2 min for clear solutions to ca. 2−10 min or more for turbid samples. Repeated titrations gave reproducible results.

Dynamic Light Scattering (QELS). All measurements were carried out at a scattering angle of 90° and at 26.0 ± 0.5 °C with a DynaPro-801 (Protein Solutions Inc., Charlottesville, VA), which employs a 30 mW solid-state 780 nm laser and an avalanche photodiode detector. Samples with 20 mM TX100 and PDADMAC of 1, 0.3, 0.1, 0.05, and 0.02 g/L in 0.10 or 0.40 M NaCl at desired Y values were prepared and were stirred for at least 2 h before measurements. The samples were introduced into the 7 μL cell through a 0.20 μm filter prior to measurement. The correlation function of the scattering data were analyzed via the method of regularization[32] and then used to determine the diffusion coefficient D of the solutes. The diffusion coefficient D can be converted into the hydrodynamic radius R_h using the Stokes−Einstein equation

$$R_h = \frac{kT}{6\pi\eta D} \tag{2}$$

where k is the Boltzmann constant, T is the absolute temperature, and η is the solvent viscosity.

Mobility Measurement. Electrophoretic mobility was measured at 26.0 ± 0.2 °C using a ZetaPALS (Brookhaven Instruments), the operation of which is based on the principles of phase analysis light scattering.[30] This technique has been described elsewhere.[16,33] The samples with 1 g/L PDADMAC and 20 mM TX100 in 0.10 M NaCl at desired Y values were stirred for at least 2 h before measurements.

Coacervate Volume Fractions. The samples of the PDADMAC/TX100-SDS systems with 2.5, 4.0, and 5.2 g/ L PDADMAC and 20 mM TX100 at $Y = 0.40$ in 0.40 M NaCl were prepared using stock solutions. Polymer molecular weights (M_n) were 9.8×10^4, 1.80×10^5, 2.16×10^5, 2.40×10^5, 2.70×10^5, 3.00×10^5, and 4.60×10^5. After the samples were stirred for at least 4 h at room temperature, centrifugation was carried at 3000 rpm and 26 °C for 1 h. After these treatments, the samples displayed two neatly separated phases. The top phases were transparent and water-like, while the bottom phases (coacervates) were translucent and gel-like. They were then stored at 26 °C. Phase separation was considered to be complete when the volumes of these two phases remained constant over 24 h. The volumes of the two phases were all recorded, and coacervate volume fraction was expressed relative to total volume.

Results

I. Coacervation Phase Behavior in 0.40 M NaCl. A. Phase Boundaries of Coacervation. Previous studies of salt effects on coacervation[16] show that coacervation takes place over a wide Y range at 0.40 M NaCl. This ionic strength facilitates the systematic study of the effects of micelle surface charge density, polymer molecular weight, and polymer/surfactant ratio on coacervation. "Type 1" turbidimetric titration curves of 1 g/L PDADMAC and 20 mM TX100 with SDS at 0.40 M NaCl are presented in Figure 1 for PDADMAC molecular weights of $M_n = 3.0 \times 10^4$, 5.8×10^4, 1.25×10^5, 1.60×10^5, 2.16×10^5, 2.70×10^5, and 4.28×10^5. The equilibrium turbidity is constant and very small at low Y values until the well-defined point of initial turbidity increase designated as Y_c, beyond which the turbidity increases gradually with increase of Y. Y_c is 0.23 independent of polymer molecular weight. For all of the systems, a maximum exists at $Y > Y_c$, which increases with polymer molecular weight. For $M_n \geq 2.70 \times 10^5$, Y_c is followed by an abrupt and dramatic increase in turbidity at $Y_{\phi 1}$, beyond which point coacervation is demonstrated by the formation of two liquid phases upon centrifugation. Further addition of SDS causes the coacervate to redissolve (at $Y_{\phi 2}$) accompanied by a decrease in turbidity. Beyond $Y_{\phi 2}$, coacervate does not exist. Thus, the interval between $Y_{\phi 1}$ and $Y_{\phi 2}$ is the coacervation region. The coacervation region increases slightly with polymer molecular weight. At $Y > Y_{\phi 2}$, the turbidity continues to decrease and then becomes constant. For $M_n \leq 2.16 \times 10^5$, no coacervation was observed. Finally, a sharp increase in turbidity signals precipitation for all the systems at Y_p, the value of which increases with polymer molecular weight. All of the turbidity values are constant with time after the system reaches equilibrium, and all of these phase boundaries are reproducible. In summary, as stated previously,[16] the above phase behavior includes a single phase in the absence of interaction between polymer and micelle, a soluble complex phase, liquid−liquid phase separation (coacervation), a soluble complex phase different from

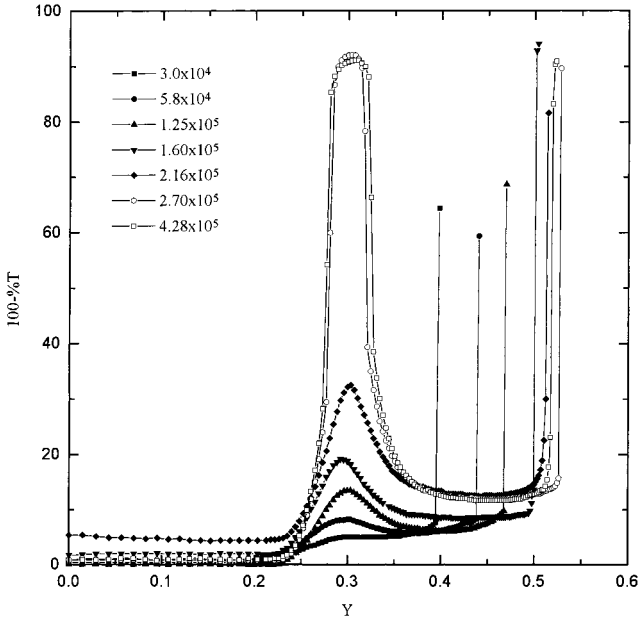

Figure 1. Equilibrium turbidity of PDADMAC/TX100-SDS as a function of Y in 0.40 M NaCl. The PDADMAC molecular weights are from 3.0×10^4 to 4.28×10^5. The concentrations of PDADMAC and TX100 are 1 g/L and 20 mM, respectively.

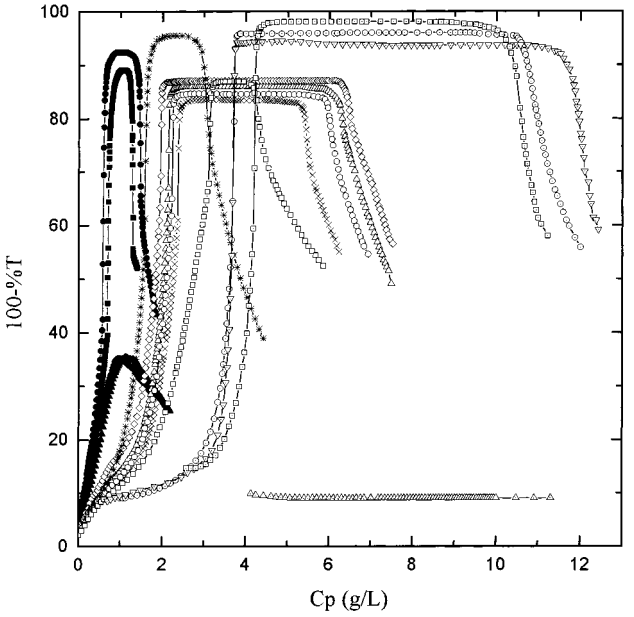

Figure 2. Equilibrium turbidity of PDADMAC/TX100-SDS in 0.40 M NaCl at $Y = 0.30$, 0.35, 0.40, and 0.50 as a function of the polymer concentration. The PDADMAC molecular weights are from 8.2×10^3 to 4.28×10^5. For $Y = 0.30$, (●) 4.28×10^5, (■) 2.70×10^5, (◆) 2.40×10^5, (▲) 2.16×10^5. For $Y = 0.40$, (◇) 2.40×10^5, (△) 2.16×10^5, (○) 1.80×10^5, (×) 9.8×10^4, (□) 5.8×10^4. For $Y = 0.50$, (▽) 3.00×10^5, (⊙) 1.80×10^5, (⊡) $= 5.8 \times 10^4$, (△) 8.2×10^3. For $Y = 0.35$, (*) 1.80×10^5.

the first one, and liquid−solid phase separation (precipitation).

The above results suggest the existence of a critical polymer MW for coacervation at any fixed polymer concentration C_p, ionic surfactant mole fraction Y, and ionic strength I and indicate that an increase in micelle surface charge density can both suppress and enhance coacervation. To investigate the relationship between the critical polymer MW, σ, and r (the mole ratio of polymer repeating units to SDS), "type 3" turbidimetric titrations were carried out by adding PDADMAC in 0.40 M NaCl to 20 mM TX100 and SDS at $Y = 0.30$, 0.40, and 0.50 also in 0.40 M NaCl. The turbidities as a function of polymer concentration are shown in Figure 2 for different PDADMAC molecular weights and different Y values. The curves are distributed among three groups for $Y = 0.30$, 0.40, and 0.50.

For $M_n = 8.2 \times 10^3$ at $Y = 0.50$, the turbidity exhibits no change over the range of C_p. For $M_n = 2.16 \times 10^5$ and 2.40×10^5 at $Y = 0.30$, a maximum is observed in each curve, but the turbidity is not large; thus, no coacervation was observed in these three cases. All other curves show a dramatic maximum. These maxima are observed at higher polymer concentration with increasing Y. At low polymer concentration, the turbidity increases gradually with addition of PDADMAC, until a sharp increase in turbidity signals the onset of coacervation at a polymer concentration defined as $C_{\phi 1}$. When sufficient polymer is added, turbidity starts to decrease as coacervate is redissolved. The point at which coacervate disappears is defined as $C_{\phi 2}$. The width of the coacervation region $C_{\phi 2} - C_{\phi 1}$ is found to increase with polymer MW. Both $C_{\phi 1}$ and $C_{\phi 2}$ can be operationally identified more precisely by differentiating the "type 3" turbidimetric curves, as described previously.[16]

As seen in Figure 2, $C_{\phi 1}$ and $C_{\phi 2}$ depend on polymer MW and SDS mole fraction Y. These coacervation phase boundaries are summarized in the three-dimensional graph of Figure 3, in which the polymer concentration is expressed as the mole ratio r of polymer repeating

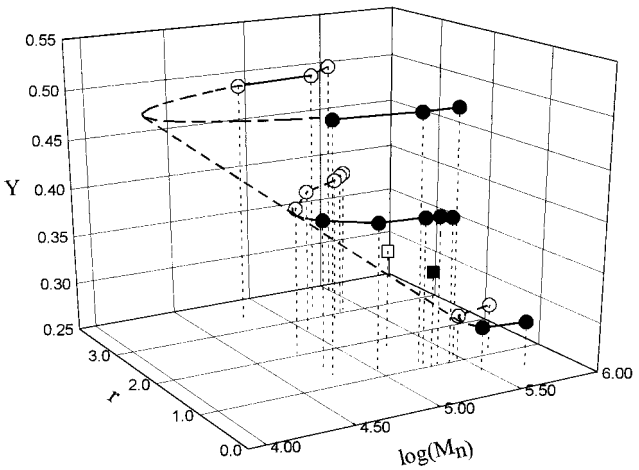

Figure 3. Phase boundaries of the PDADMAC/TX100-SDS system in 0.40 M NaCl. r is the bulk molar ratio of polyelectrolyte repeating units to SDS. The filled and open symbols represent the complexes with negative and positive charges, respectively. The region between the two surfaces is coacervation.

units to SDS. This ratio is dependent on both polymer concentration and Y. Filled and open symbols represent initial and terminal points for coacervation during "type 3" titrations, respectively. Thus, the coacervation region is situated between the two surfaces comprised respectively of filled and open symbols. As observed in Figure 3, the size of the coacervation region diminishes with a decrease in polymer molecular weight and finally disappears (the dashed lines are used to see the tendency more clearly). The size of the coacervation region increases with increase of Y and MW. It is also found that higher polymer-to-surfactant ratio is required for coacervation at higher Y.

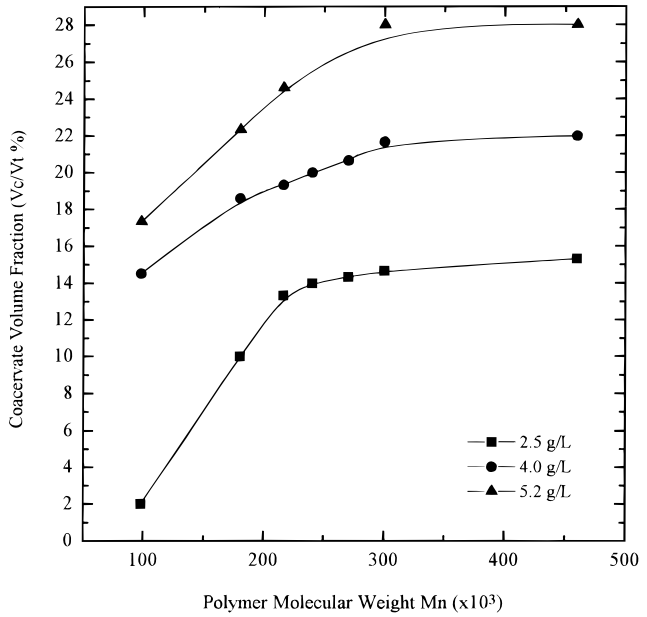

Figure 4. Coacervate volume fraction for PDADMAC/TX100-SDS system at $Y = 0.40$ in 0.40 M NaCl as a function of polymer molecular weight. V_c and V_t are volumes of coacervates and total solutions, respectively. The PDADMAC concentrations corresponding to the three curves are 2.5, 4.0, and 5.2 g/L.

The phase boundaries in Figure 3 suggest that coacervation can be both induced and suppressed by changing Y and r. For example, a TX100-SDS solution at $Y = 0.35$ in 0.40 M NaCl at $r = 0$ is located outside the surface formed by filled symbols. Upon adding PDADMAC, r is increased until coacervation takes place at the point indicated by "■", which is located on the filled-symbol surface. A further increase of r results in coacervation redissolution at point "□", which is on the open-symbol surface. In summary, according to Figure 3, coacervation can be induced or suppressed by leading the system into or out of the coacervation region through changing polymer molecular weight, micelle charge density, or polymer-to-surfactant ratio.

B. Coacervate Volume Fraction. Coacervate volume fractions of PDADMAC/TX100-SDS in 0.40 M NaCl as a function of PDADMAC molecular weight are presented in Figure 4. The concentration of TX100 is 20 mM, and the SDS mole fraction Y is 0.40, so the total surfactant concentration is fixed. The three curves correspond to polymer concentrations of 2.5, 4.0, and 5.2 g/L.

These coacervate volume fraction curves contain two common traits: a rapid increase of coacervate volume fraction with polymer molecular weight at low MW and a roughly constant coacervate volume fraction at higher polymer molecular weight. For a given MW, coacervate volume fraction increases with increase in polymer concentration, i.e., with an increase in polymer-to-surfactant ratio. Clearly, both polymer molecular weight and stoichiometry affect coacervate volume fraction significantly.

II. Structure of Soluble Complexes in 0.10 M NaCl and 0.40 M NaCl. Structural information on complexes and coacervates from dynamic light scattering and mobility measurements may help to understand the above phase behavior. Figure 3 shows that coacervation occurs over a wide range for high polymer molecular weight. Therefore, complex size and mobility

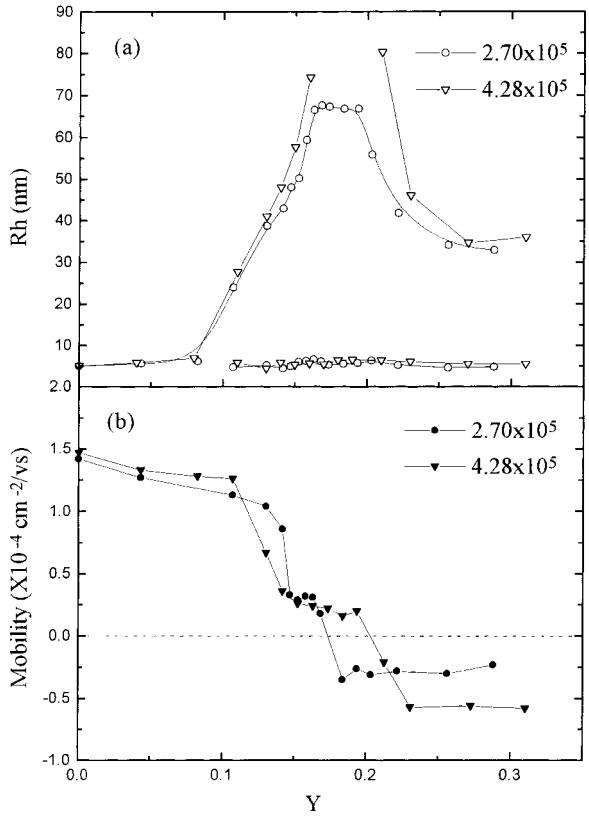

Figure 5. (a) Radius and (b) mobility of PDADMAC/TX100-SDS in 0.10 M NaCl as a function of Y. The concentrations of PDADMAC ($M_n = 2.70 \times 10^5$, 4.28×10^5) and TX100 are 1 g/L and 20 mM. QELS yields a bimodal size distribution in (a): the lower curve is the contribution from uncomplexes micelle, while the upper curve shows the contribution from complex.

were studied as a function of Y for 1 g/L PDADMAC with $M_n = 4.28 \times 10^5$ and 20 mM TX100 in 0.10 M NaCl with the results shown in Figure 5a,b. To compare the situation for different polymer molecular weights, previous results for PDADMAC with $M_n = 2.70 \times 10^5$ are also included. Although the phase boundaries were obtained at $I = 0.40$ M, such high ionic strength leads to difficulties with the mobility technique. While the condition $I = 0.10$ M does not match that of the phase boundaries, the results still give useful structural information. At $Y < Y_c$, the size is almost constant, and the mobility decreases only slightly with Y, indicating that no interaction take place between polymer and micelles. Because the polymer concentration is very low relative to TX100, the small value of R_h arises mainly from the scattering of mixed micelles. Since micelles are nearly uncharged at low Y, the observed large positive mobility is mainly due to PDADMAC. The slight decrease in mobility at $0 < Y < 0.1$ is from the contribution of mixed TX100-SDS micelles which contain a very small fraction of SDS in this region. With a further addition of SDS, a sharp increase in size and a marked decrease in absolute mobility are observed, providing strong evidence of the formation of a complex whose mobility is positive. QELS yields a bimodal size distribution: in Figure 5a, the lower curve is the contribution from uncomplexed micelles, which remains essentially unchanged, while the upper curve shows that R_h of the complex changes with Y. In the coacervation range, the mobility approaches zero, and the size of the complex becomes very large, increasing with an increase in

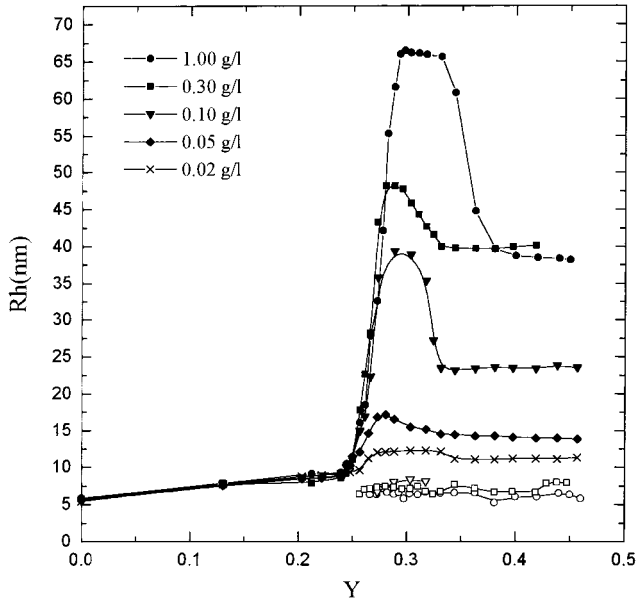

Figure 6. Radius of the systems of PDADMAC ($M_n = 2.70 \times 10^5$)/TX100-SDS as a function of Y in 0.40 M NaCl at PDADMAC concentrations of 1.00, 0.30, 0.10, 0.05, and 0.02 g/L. QELS yields a bimodal size distribution: the lower curve is the contribution from uncomplexed micelle, while the upper curve shows the contribution from complex.

polymer molecular weight. Further addition of SDS leads to a significant decrease in size while the mobility becomes negative. When $Y \geq Y_p$, neither size nor mobility can be measured because of limitations of the techniques in systems of large particles. These results indicate that mobility is close to zero when coacervation takes place, regardless of polymer molecular weight.

Figure 6 shows complex size as a function of Y in 0.40 M NaCl and 20 mM TX100 at varying polymer concentration C_p of 0.02−1.0 g/L. In this polymer concentration range, no change in size is observed until Y reaches $Y_c = 0.23$, beyond which complex size starts to increase. For $C_p = 0.02$ and 0.05 g/L, the slight increase in size suggests that only intrapolymer complexes are formed at such low C_p. In the cases of 0.10, 0.30, and 1.00 g/L polymer concentrations, a bimodal size distribution exists as in Figure 5. The upper curves show significant increases in size, which provides evidence that interpolymer complexes are formed when C_p is high enough. For $C_p = 0.30$ and 1.00 g/L, coacervation was observed in the Y ranges 0.27−0.33 and 0.27−0.35, respectively, but no coacervation was observed at $C_p = 0.10$ g/L. As Y continues to increase, the size begins to decrease, finally becoming constant, at which point the coacervate was redissolved. These results suggest a minimum complex size for coacervation, about 45 nm in the present system.

Discussion

Effect of Micelle Surface Charge Density. Since TX100-SDS mixed micelle surface charge density is proportional to the mole fraction of ionic surfactant, i.e., Y, the effect of Y can be thought of as the effect of micelle surface charge density σ.

The phase behavior in the PDADMAC/TX100-SDS system, including complex formation, coacervation, and precipitation, results from the binding of anionic micelles to cationic polymers, a consequence of electrostatic attractive interactions. Veis and Aranyi[34] proposed that complex coacervation between oppositely charged macromolecules occurred in two steps. First, macroions aggregate by electrostatic interaction to form neutral aggregates of low configurational entropy, and then these aggregates rearrange to form coacervate. On the basis of this theory for the polyelectrolyte−polyelectrolyte system, we put forward in ref 16 a simple mechanism for polyelectrolyte−micelle coacervation. This mechanism can be used to interpret the phase behavior of PDADMAC/TX100-SDS systems with higher polymer molecular weights seen in Figure 1.

The processes of macroionic aggregation to yield neutral proto-coacervate could in fact be observed by dynamic and electrophoretic light scattering, although instrumental limitations with the latter made it necessary to conduct these measurements in 0.10 M NaCl. In Figure 5, one observes a single phase without complexes at $Y < Y_c$ under which conditions the surface charge density of the TX100-SDS mixed micelles σ is not sufficient to lead to complex formation. Thus, turbidity, radius, and mobility all remain unchanged. In the region of $Y > Y_c$ but before coacervation, σ increases with the addition of SDS, which leads to soluble complex formation, as indicated by an increase in size and turbidity and a decrease in absolute mobility. In this region, complexes carry net positive charges. With further addition of SDS, progressively higher σ causes more mixed micelles to bind, accompanied by a prominent increase in size and turbidity and a decrease in absolute mobility. Here, complex charges are electrically neutralized, which enables intrapolymer complexes to aggregate into interpolymer complexes, which in turn form coacervate. Thus, the coacervation region is centered at the charge neutralization point. With the addition of SDS beyond charge neutralization, higher σ increases the intrinsic binding of micelles to polyelectrolytes but also eventually produces electrostatic intermicellar repulsion and concomitant intercomplex repulsion. These two effects eventually lead to a redissolution of the interpolymer complexes into intrapolymer complexes with net negative charge, which corresponds to the soluble complex region located between coacervation and precipitation. The electrostatic intermicellar repulsion could also cause the number of mixed micelles bound per polymer chain ($\bar{n}$) to decrease. The fact that the mobility in this region is almost unchanged with addition of SDS might arise from the compensating effects of a decrease in $\bar{n}$ simultaneous with an increase in Y. At $Y > Y_p$, mixed micelles with very high charge density display a strong interaction with the polyelectrolytes, leading to tight binding of micelles with polyelectrolytes. With the consequent loss of counterions and hydration, precipitation occurs.

The effects of polymer concentration at constant σ are shown in the "type 3" turbidimetric titration results in Figure 2. For a given polymer MW, the coacervation region widens with the increase of Y. This result can be easily interpreted using the mobility results. According to Figure 5, the mobility is close to zero when coacervation takes place. It can be deduced that the soluble complexes at $C_p < C_{\phi 1}$ and $C_p > C_{\phi 2}$ carry negative and positive charges, respectively. At $C_p > C_{\phi 1}$, the addition of polymer neutralizes intrapolymer complexes with negative charges by decreasing the average number of micelles bound per polymer chain. Aggregation of neutralized complexes allows coacervation to take place with accompanying extremely large turbidity.

Upon a further addition of polymer, each polymer chain will bind on average a decreasing number of micelles, eventually causing coacervates to disaggregate into positively charged intrapolymer complexes with a corresponding decrease in turbidity. At higher micelle charge density, more polymers are needed to neutralize the complexes to reach the requirement of coacervation. After coacervation, the interpolymer aggregates containing micelles of larger σ can contain more polymers before the coacervate is redissolved into positively charged intrapolymer complexes. As a result, the coacervation region is wider and shifted toward a higher polymer concentration with increase in Y.

Effect of Polyelectrolyte Molecular Weight. Figure 1 shows that a minimum polymer molecular weight is required for coacervation at a given polymer concentration. This result can be explained in a zeroth-order way by polymer phase separation theory. The purpose of the following model is not a rigorous theoretical treatment. However, we believe that some elements of such a simplified approach can be useful to understand coacervation. According to Flory−Huggins theory,[35,36] the chemical potential of solvent in a polymer solution relative to the pure solvent as standard state can be written

$$\mu_1 - \mu_1^0 = RT[\ln(1 - v_2) + (1 - 1/x)v_2 + \chi_1 v_2^2] \quad (3)$$

where v_2, x, and χ_1 denote volume fraction of polymer solute, number of structural repeating units of per polymer chain (proportional to polymer molecular weight), and polymer−solvent interaction free energy parameter, respectively. Then, the critical polymer volume fraction v_{2c} (polymer solubility) at which phase separation appears is determined by x and χ_1, i.e., by polymer molecular weight and solvent−polymer interaction parameter. v_{2c} may be expressed by the following equations:

$$v_{2c} = 1/(1 + x^{1/2}) \approx 1/x^{1/2} \quad (4)$$

and

$$v_{2c}^3 = (1 - 1/\sqrt{2\chi_1})/x \quad (5)$$

which means that polymer solubility decreases with increasing x and increasing χ_1.

Piculell and co-workers[8] rationalized phase separation of complexes of polymers with oppositely charged surfactants by considering the complex as a single quasi-component with a variable composition, which could then display varying solubility. Similarly, because the complex is a precursor of coacervation, we consider the polymer−micelle complex as a kind of polymer, wherein one bound micelle along with a certain number of polymer residues (n_p) can be thought as a structural "repeating unit". Then, x can be expressed as

$$x = \frac{\mathrm{MW}}{m_0 n_p} \quad (6)$$

where m_0 is the weight per monomer residue in the polymer molecule.

Systems containing charged species in principle exceed the limitations of the Flory−Huggins theory, because the interaction energy term χ_1 is based on short-range interaction, while electrostatic interactions are typically long-range. Thalberg and co-workers[25] used a mean-field approximation with five effective interaction parameters to calculate phase diagrams and indicated that the Flory−Huggins theory can account for the phase behavior observed in a polyelectrolyte−surfactant system. Furthermore, if the ionic strength is large enough and if there is sufficient intracomplex charge neutralization, the long-range interaction may be suppressed. In the present case, the ionic strength is 0.40 M, and the complexes are close to charge neutrality when coacervation takes place, so we think that the Flory−Huggins theory can be invoked to understand the effect of MW on coacervation. We assume that the interaction energy term χ_1 of the "repeating units" in the complexes decreases with decrease in their net charge density. Therefore, complexes of higher polymer MW and lower net charge density tend to phase separate from the complex solution (coacervation). If the polymer MW is low enough or complex net charge density is large enough, coacervation cannot take place. In other words, a minimum polymer MW and a maximum χ_1 are required for coacervation.

Overbeek and Voorn[21] obtained critical conditions for complex coacervation of symmetrical polyions in salt-free systems as $\sigma_p^3 r_p \geq 0.5$, where σ_p and r_p are polymer charge density and the number of polymer repeat units, respectively. This condition also suggests that no coacervate forms at sufficiently low r_p (proportional to polymer MW) when the polymer charge density is constant. This tendency is consistent with the present result.

Since polymer charge density is independent of polymer MW, χ_1 of the complex is also independent of MW. So the effect of MW on coacervation must be through x, which also determines the size of the complex, and a minimum x would correspond to some minimum complex size. The results from Figure 6 appear to suggest that 45 nm is the size of the complex which is the precursor of coacervation in the present system,[37,38] i.e., $R_h = 45$ nm when x attains a critical value x_c for phase separation (coacervation). The size of complexes increases with increasing (uncomplexed) polymer MW (Figure 5a). The resulting large intrapolymer complexes aggregate more readily into interpolymer complexes leading to coacervation,[23,27,28,37] presumably because the gain in entropy when complexes rearrange into a randomly distributed coacervate phase[39] is enhanced with increasing polymer MW. Because a complex involving one chain of MW = M' is thermodynamically the same as a complex comprising two chains with MW = $M'/2$, one may speculate that coacervation could take place without interpolymer complex formation if an intrapolymer complex were large enough to attain x_c.

Complexes formed from higher molecular weight polymer can attain this condition over a broad range of conditions and so widen the coacervation region at a given Y, as shown in Figure 3. This result can be represented by the schematic diagram of Figure 7. The coacervation region is centered at the charge neutralization point. Phase separation (coacervation) depends on the combined effects of charge neutrality and large complex size. With increase of polymer MW, larger complexes can coacervate even when the complex net charge departs somewhat from zero, while smaller complexes cannot coacervate even if their charges are neutralized. Thus, the width of the coacervation region increases with increasing polymer MW.

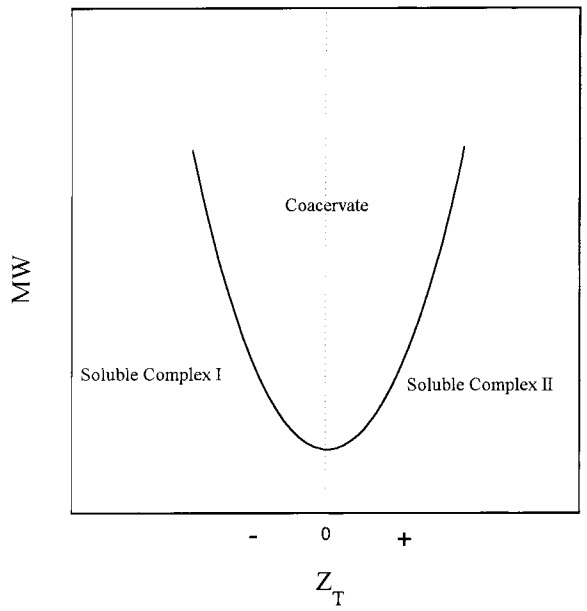

Figure 7. Schematic description of coacervation region dependence on polymer molecular weight and net charge of complex.

Polymer MW also affects the quantity of coacervate as predicted by Voorn and Overbeek.[21] The coacervate volume fraction for the PDADMAC/TX100-SDS system exhibits a similar tendency, as shown in Figure 4. At constant polymer concentration, coacervate volume fraction increases rapidly with PDADMAC molecular weight at MW $< 2 \times 10^5$, whereas the coacervate volume fraction is almost constant at higher MW. These results are consistent with the preceding discussion of x_c. In the range of higher polymer MW, all polymer molecules can lead to complexes that satisfy $x > x_c$, so no obvious differences in coacervate volume fraction could be observed in the high MW range.

Effect of Polyelectrolyte-to-Surfactant Ratio. The importance of charge neutrality leads to an effect of the polyelectrolyte-to-SDS ratio, r. At fixed total surfactant concentration, r depends on polymer concentration C_p and on Y. The values of r, Y, and MW determine the number of micelles bound per polymer chain $\bar{n}$. Then, the critical supramolecular parameters of the complex including the net charge Z_T (which controls χ_1) and the size R (related to x) are determined by r, Y, and MW. The three-dimensional coacervation phase boundary in Figure 3 presents the effect of r on coacervation and its relationship with micelle surface charge density and polymer molecular weight. This figure suggests that both high and low r can suppress coacervation.

From Figure 3, it is noted that the value of r producing maximum coacervation increases with increasing Y, the width of this region increasing also. The requirement of charge neutrality can be used to explain this as shown by the schematic in Figure 8. Coacervation takes place when the net charge of the complexes Z_T is located between Z_1 and Z_2. The two lines represent hypothetical relationships between the net complex charge and r at low and high Y, respectively. The binding constant of micelles to polyelectrolytes must increase strongly with Y.[28] Thus, although the number of micelles bound per polymer chain $\bar{n}$ varies inversely with r for stoichiometric reasons, the dependence of $\bar{n}$ on Y is much greater than its dependence on r. At any

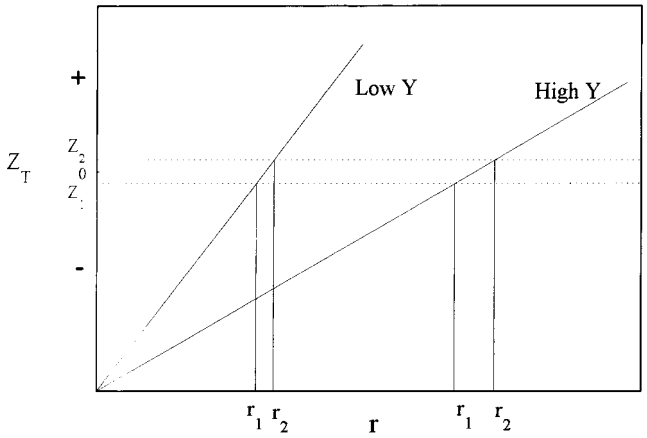

Figure 8. Schematic description of coacervation region with respect to r and Y. When the net charge of complexes Z_T is located in the charge region between Z_1 and Z_2, coacervation takes place. The region between r_1 and r_2 is the coacervation region.

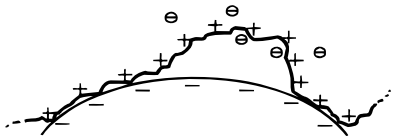

Figure 9. Schematic of a representative part of a structural unit within a complex. A local charge excess of polymer segments is compensated by its counterions.

r value, Z_T is more negative for larger Y. dZ_T/dr, the change of net complex charge with r, decreases with increasing Y. Therefore, the coacervation region $r_1 < Y < r_2$ is larger at higher Y, and the coacervation region moves to high r at high Y.

Figure 3 shows that coacervation almost always requires $r > 1$, which means that the number of polymer charge units in the complexes is probably more than that of SDS. When coacervation takes place, the complexes, composed of polymer, micelles, and counterions, have mobility close to zero. Owing to limitations of polymer chain flexibility, micelle geometry, and intermicellar repulsion, some of the charge units on the polymer chain cannot be locally neutralized by micellar SDS and must be neutralized by the counterion Cl^- (see Figure 9). Coacervation thus occurs at $r > 1$.

The coacervate volume fraction is also affected by r. In Figure 4, $C_p = 2.5$, 4.0, and 5.2 g/L corresponds to $r = 1.19$, 1.91, and 2.48, respectively, indicating that coacervate volume fraction increases with r. In Figure 3, the systems with $r = 1.19$ and 2.48 are located at the initiation and termination of the coacervation region. At a given surfactant concentration, the larger coacervate volume fraction at higher r means that an increase in the amount of polymer bound to micelles leads to enhanced coacervate volume fraction.

Conclusions

Turbidity, dynamic light scattering, and electrophoretic mobility have been used to study the effects of micelle surface charge density, polymer molecular weight, and polyelectrolyte-to-surfactant ratio on coacervation of the PDADMAC/TX100-SDS system. The coacervate volume fraction was also studied as a function of polymer molecular weight. These results indicate that complex charge near neutrality and a minimum complex size about 45 nm are required for coacervation to occur.

The size of coacervation region widens with increasing polymer molecular weight and micelle charge density over the range studied. Both lower and higher polyelectrolyte-to-surfactant ratio can suppress coacervation. Coacervate volume fraction increases with an increase of polymer molecular weight and with an increase in polyelectrolyte-to-surfactant ratio in the coacervation region. A further study on the effects of micelles size is in progress.

Acknowledgment. This work was supported by NSF (DMR-9619722) and a grant from the Procter & Gamble Company.

References and Notes

(1) Piculell, L.; Lindman, B. *Adv. Colloid Interface Sci.* **1992**, *41*, 149.
(2) Guillemet, F.; Piculell, L. *J. Phys. Chem.* **1995**, *99*, 9201.
(3) Ranganathan, S.; Kwak, J. C. T. *Langmuir* **1996**, *12*, 1381.
(4) Lindman, B.; Thalberg, K. In *Interaction of Surfactants with Polymers and Proteins*; Goddard, E. D., Ananthapadmanabhan, K. P., Eds.; CRC Press: Boca Raton, FL, 1993; Chapter 5.
(5) Li, Y.; Dubin, P. L. In *Structure and Flow in Surfactant Solutions*; Herb, C. A., Prud'homme, R. K., Eds.; ACS Symposium Series 578; American Chemical Society: Washington, DC, 1994; Chapter 23, p 320.
(6) Goddard, E. D. *Colloids Surf.* **1986**, *19*, 301.
(7) Hayakawa, K.; Kwak, J. C. T. In *Cationic Surfcatant. Physical Chemistry*; Rubingh, D. N., Holland, P. M., Eds.; Marcel Dekker: New York, 1991; p 189.
(8) Piculell, L.; Lindman, B.; Karlström, G. In *Polymer-Surfactant Systems*; Kwak, J. C. T., Ed.; Marcel Dekker: Basel, 1998; p 65.
(9) Schmitt, C.; Sanchez, C.; Desobry-Banon, S.; Hardy, J. *Crit. Rev. Food Sci. Nutr.* **1998**, *38*, 689.
(10) Burgess, D. J. In *Macromolecular Complexes in Chemistry and Biology*; Dubin, P. L., Bock, J., Davis, R., Thies, C., Eds.; Springer-Verlag: Berlin, 1994; p 285.
(11) Bungenberg de Jong, H. G. In *Colloid Science*; Kruyt, H. R., Ed.; Elsevier: Amsterdam, 1949; Vol. 2.
(12) Thalberg, K.; Lindman, B.; Karlström, G. *J. Phys. Chem.* **1991**, *95*, 6004.
(13) Goddard, E. D. *J. Soc. Cosmet. Chem.* **1990**, *41*, 23.
(14) Kayes, J. B. *J. Pharm. Pharmacol.* **1977**, *29*, 163.
(15) Deasy, P. B. In *Microencapsulation and Related Drug Process*; Marcel Dekker: Basel, 1984.
(16) Wang, Y.; Kimura, K.; Huang, Q.; Dubin, P.; Jaeger, W. *Macromolecules* **1999**, *32*, 7128.
(17) Dubin, P. L.; Oteri, R. *J. Colloid Interface Sci.* **1983**, *95*, 453.
(18) Dubin, P. L.; Curran, M. E.; Hua, J. *Langmuir* **1990**, *6*, 707.
(19) McQuigg, D. W.; Kaplan, J. I.; Dubin, P. L. *J. Phys. Chem.* **1992**, *96*, 1973.
(20) Goddard, E. D.; Hannan, R. B. *J. Colloid Interface Sci.* **1976**, *55*, 73.
(21) Overbeek, J. T. G.; Voorn, M. J. *J. Cell. Comput. Physiol.* **1957**, *49* (Suppl. 1), 7.
(22) Thalberg, K.; Lindman, B.; Karlström, G. *J. Phys. Chem.* **1991**, *95*, 3370.
(23) Li, Y.; Xia, J.; Dubin, P. L. *Macromolecules* **1994**, *27*, 7049.
(24) Goddard, E. D.; Hannan, R. B. *J. Am. Oil Chem. Soc.* **1977**, *54*, 561.
(25) Thalberg, K.; Lindman, B.; Karlström, G. *J. Phys. Chem.* **1990**, *94*, 4289.
(26) Dubin, P. L.; Rigsbee, D. R.; McQuigg, D. W. *J. Colloid Interface Sci.* **1985**, *105*, 509.
(27) Li, Y.; Dubin, P. L.; Dautzenberg, H.; Lück, U.; Hartmann, J.; Tuzar, Z. *Macromolecules* **1995**, *28*, 6795.
(28) Xia, J.; Zhang, H.; Rigsbee, D. R.; Dubin, P. L.; Shaikh, T. *Macromolecules* **1993**, *26*, 2759.
(29) Rigsbee, D. R.; Dubin, P. L. *Langmuir* **1996**, *12*, 1928.
(30) Miller, J. F.; Schätzel, K.; Vincent, B. *J. Colloid Interface Sci.* **1991**, *143*, 532.
(31) Dautzenberg, H.; Görnitz, E.; Jaeger, W. *Macromol. Chem. Phys.* **1998**, *199*, 1561.
(32) Provencher, S. W. *Comput. Phys. Commun.* **1982**, *27*, 229.
(33) Tscharnuter, W. W.; McNeil-Watson, F.; Fairhurst, D. In *Particle Size Distribution III: Assessment and Characterization*; Provder, T., Ed.; ACS Symposium Series 693; American Chemical Society: Washington, DC, 1996; Chapter 23, p 327.
(34) Veis, A.; Aranyi, C. *J. Phys. Chem.* **1960**, *64*, 1203.
(35) Flory, P. J. In *Principles of Polymer Chemistry*; Cornell University Press: Ithaca, NY, 1953.
(36) Huggins, M. L. In *Physical Chemistry of High Polymers*; John Wiley & Sons: New York, 1958.
(37) Li, Y.; Dubin, P. L.; Havel, H. A.; Edwards, S. L.; Dautzenberg, H. *Langmuir* **1995**, *11*, 2486.
(38) Dubin, P. L.; Thé, S. S.; Gan, L. M.; Chew, C. H. *Macromolecules* **1990**, *23*, 2500.
(39) Veis, A.; Bodor, E.; Mussell, S. *Biopolymers* **1967**, *5*, 37.

MA991886Y